British Journal of Pharmacology (2006) 148, 264–273
www.nature.com/bjp

Inhibition of TRPM2 cation channels by *N*-(*p*-amylcinnamoyl)anthranilic acid

[1,3]Robert Kraft, [1,2]Christian Grimm, [1,2]Henning Frenzel & *,[1]Christian Harteneck

[1]Institut für Pharmakologie, Charité Campus Benjamin Franklin, Thielallee 69-73, Berlin 14195, Germany and [2]Fachbereich Biologie, Chemie, Pharmazie, Freie Universität Berlin, Takustr. 3, Berlin 14195, Germany

1 TRPM2 is a Ca^{2+}-permeable nonselective cation channel activated by intracellular ADP-ribose (ADPR) and by hydrogen peroxide (H_2O_2). We investigated the modulation of TRPM2 activity by *N*-(*p*-amylcinnamoyl)anthranilic acid (ACA). ACA has previously been reported to inhibit phospholipase A_2 (PLA_2).

2 Using patch-clamp and calcium-imaging techniques, we show that extracellular application of 20 μM ACA completely blocked ADPR-induced whole-cell currents and H_2O_2-induced Ca^{2+} signals ($IC_{50} = 1.7\,\mu M$) in HEK293 cells transfected with human TRPM2. Two other PLA_2 inhibitors, *p*-bromophenacyl bromide (BPB; 100 μM) and arachidonyl trifluoromethyl ketone (20 μM), had no significant effect on ADPR-stimulated TRPM2 activity.

3 Inhibition of TRPM2 whole-cell currents by ACA was voltage independent and accelerated at decreased pH. ACA was ineffective when applied intracellularly. The single-channel conductance was not changed during ACA treatment, suggesting a reduction of TRPM2 open probability by modulating channel gating.

4 ACA (20 μM) also blocked currents through human TRPM8 and TRPC6 expressed in HEK293 cells, while BPB (100 μM) was ineffective. TRPC6-mediated currents ($IC_{50} = 2.3\,\mu M$) and TRPM8-induced Ca^{2+} signals ($IC_{50} = 3.9\,\mu M$) were blocked in a concentration-dependent manner.

5 ADPR-induced currents in human U937 cells, endogeneously expressing TRPM2 protein, were fully suppressed by 20 μM ACA.

6 Our data indicate that ACA modulates the activity of different TRP channels independent of PLA_2 inhibition. Owing to its high potency and efficacy ACA can serve, in combination with other blockers, as a useful tool for studying the unknown function of TRPM2 in native cells.
British Journal of Pharmacology (2006) **148,** 264–273. doi:10.1038/sj.bjp.0706739;
published online 10 April 2006

Keywords: ADP-ribose; flufenamic acid; hydrogen peroxide; TRPM channels; U937

Abbreviations: $AACOCF_3$, arachidonyl trifluoromethyl ketone; ACA, *N*-(*p*-amylcinnamoyl)anthranilic acid; BAPTA, 1,2-bis(2-aminophenoxy)ethane-*N*,*N*,*N*′,*N*′-tetraacetic acid; BPB, *p*-bromophenacyl bromide; HEK293, human embryonic kidney; NMDG, *N*-methyl-D-glucamine; ROS, reactive oxygen species; TRP, transient receptor potential

Introduction

TRPM2 belongs to the melastatin-related proteins within the transient receptor potential (TRP) superfamily of nonselective cation channels (Fleig & Penner, 2004; Kraft & Harteneck, 2005). TRPM2 has been reported to be highly expressed in brain (Nagamine *et al*., 1998; Hara *et al*., 2002), where it is preferentially localized in microglial cells, the host macrophages of the central nervous system (Kraft *et al*., 2004). An expression of TRPM2 in immune cells in general is suggested by its detection in some T-lymphocyte cell lines (Sano *et al*., 2001; Hara *et al*., 2002), monocytic U937 cells (Perraud *et al*., 2001; Sano *et al*., 2001) and primary human neutrophils (Heiner *et al*., 2003a). Besides the expression in immunocytes, TRPM2 could be identified in insulinoma cell lines (Hara *et al*., 2002; Inamura *et al*., 2003). A cation current with TRPM2-like properties has been described in rat striatal neurons (Smith *et al*., 2003; Hill *et al*., 2006), and a TRPM2 splice variant was exclusively found in human striatum (Uemura *et al*., 2005). TRPM2 is activated by intracellular ADP-ribose (ADPR) (Perraud *et al*., 2001; Sano *et al*., 2001) and reactive oxygen species (ROS) such as hydrogen peroxide (H_2O_2) (Hara *et al*., 2002; Wehage *et al*., 2002). Opening of TRPM2 channels by H_2O_2 has been suggested to depend on activation of poly(ADPR) polymerase (Fonfria *et al*., 2004), an ubiquitously expressed enzyme catalyzing the breakdown of NAD^+ into nicotinamide and ADPR. Furthermore, TRPM2 activity is increased at elevated intracellular Ca^{2+} concentrations ($[Ca^{2+}]_i$) (McHugh *et al*., 2003). Arachidonic acid, a phospholipase A_2 (PLA_2) metabolite, has been shown to potentiate Mn^{2+} influx in TRPM2-expressing cells (Hara *et al*., 2002). However, for most TRP channels including TRPM2, the range of pharmacological modulators of TRPM2 is limited. Only recently, flufenamic acid (FFA) and the imidazole antifungal agents clotrimazole and econazole have been described as TRPM2 blockers (Hill *et al*., 2004a, b).

An involvement of TRPM2 in the Ca^{2+} signalling of brain macrophages was suggested from experiments in primary

*Author for correspondence; E-mail: Christian.Harteneck@charite.de
[3]Current address: Carl-Ludwig-Institut für Physiologie, Universität Leipzig, Liebigstr. 27, Leipzig 04103, Germany.

cultured rat microglia showing large ADPR- and H_2O_2-induced cation currents and a strong Ca^{2+} influx (Kraft *et al*., 2004). RIN-5F insulinoma cells showed a TRPM2-mediated Ca^{2+} entry in response to treatment with H_2O_2 and tumor necrosis factor-α (Hara *et al*., 2002). In this context, TRPM2 has been proposed to confer susceptibility to cell death (Hara *et al*., 2002; Zhang *et al*., 2003; Fonfria *et al*., 2004; 2005). Alternatively, TRPM2 has been discussed as a candidate for a ROS-induced Ca^{2+}-entry pathway in macrophages, acting as a positive feedback loop enhancing Ca^{2+}-dependent H_2O_2 generation (Heiner *et al*., 2003b; Kraft *et al*., 2004; Perraud *et al*., 2004). Pharmacological manipulation of the cellular concentrations of ADPR or arachidonic acid, together with the discovery and use of direct channel inhibitors may help to investigate the role of TRPM2 in biological processes.

This study was originated to investigate the effects of PLA_2 modulation on TRPM2 activity. To our surprise, 20 μM of the PLA_2 inhibitor *N*-(*p*-amylcinnamoyl)anthranilic acid (ACA) led to a rapid and complete suppression of recombinant and native human TRPM2 channels. ACA has previously been described to reduce arachidonic acid accumulation in glucose-stimulated rat pancreatic islet cells (Konrad *et al*., 1992) and to mimic the effect of antisense nucleotide treatment against cytoplasmic PLA_2 on Ca^{2+}-evoked exocytosis in insulinoma cells (Olsen *et al*., 2003). A direct modulation of ion channels by ACA has not been reported so far.

Methods

Cell culture and transfection

HEK293 cells were cultured in minimum essential medium, supplemented with 10% FBS, 0.2 mM L-glutamine, 100 U ml^{-1} penicillin and 100 U ml^{-1} streptomycin under 5% CO_2 atmosphere at 37°C. The cDNAs of the following TRP channels were used for experiments: hTRPM2 (GenBank number AY026252), hTRPM8 (GenBank number NM024080) and hTRPC6 (GenBank number NM004621). Cells were plated onto glass coverslips and transfected with 1–2 μg of plasmid DNA using 5 μl of FUGENE 6 transfection reagent (Roche, Indianapolis, IN, U.S.A.) and 95 μl of OptiMEM medium (Invitrogen, Groningen, The Netherlands) 1 or 2 days later. Electrophysiological studies and calcium-imaging experiments were carried out 1–2 days after transfection. U937 human myeloid leukemia cells were cultured in RPMI 1640 medium, supplemented with 10% FBS, 0.2 mM L-glutamine, 100 U ml^{-1} penicillin and 100 U ml^{-1} streptomycin under 5% CO_2 atmosphere at 37°C. Cells were plated onto glass coverslips 1–4 h before patch-clamp experiments.

Western blot

For generation of polyclonal rabbit antisera, three rabbits were immunized with a peptide–KLH conjugate. The peptide sequence was delineated from the N-terminus of TRPM2 (NH_2-MEPSALRKAGSEQEEC-$CONH_2$). Antisera were tested beginning with day 90 after immunization. The whole antiserum was isolated at day 150, and the specific IgG fraction was isolated by affinity column purification (Pineda Antikörper-Service, Berlin, Germany). Membrane fractions extracted from the human cell lines (U937, HL-60, MEG-01 and HEK293) and TRPM2- or TRPM3-transfected HEK293 cells were separated on a 6% polyacrylamide gel. The proteins were transferred on nitrocellulose membranes, and the presence of the TRPM2 protein was analyzed by incubating the membrane with an antibody diluted 1 : 2000 at 4°C overnight. On the next day, the membranes were washed, and the bound antibody was detected using an ECL Advance Western Blotting Detection kit (Amersham Biosciences, Freiburg, Germany).

Electrophysiology

Cells were placed in a recording chamber (chamber volume ~0.5 ml) connected to a solution drain driven by gravity feed at a rate of 4 ml min^{-1}. To accelerate complete solution exchanges, the solution volume was reduced to ~0.1 ml before adding another solution. Membrane currents were measured in the whole-cell configuration of the patch-clamp technique. Currents were recorded using an Axopatch 200B amplifier (Axon Instruments, CA, U.S.A.), subsequently low-pass filtered at 1 kHz or 500 Hz, digitized with a sampling rate of 5 kHz or 500 Hz and analyzed using pCLAMP software (version 7.0; Axon Instruments). The pipette resistance varied between 3 and 5 MΩ. Most currents were elicited by voltage ramps from −100 to +100 mV (400 ms duration) applied every 2 s from a holding potential of 0 mV. For experiments on TRPM2-transfected HEK293 cells and on U937 cells, pipettes were filled with a solution composed of 50 mM $CsCH_3O_3S$, 25 mM CsCl, 10 mM 1,2-bis(2-aminophenoxy)ethane-*N*,*N*,*N*′,*N*′-tetraacetic acid (BAPTA), 8.3 mM $CaCl_2$, 4 mM Na_2ATP, 2 mM $MgCl_2$ and 10 mM HEPES (pH 7.2 with ~52 mM CsOH). The concentration of free Ca^{2+} in this solution was calculated to be ~600 nM using the software WinMAXC (v.2.05; Chris Patton, Stanford, CA, U.S.A.). To induce activation of TRPM2 channels, the pipette solution contained 1 mM ADPR. For all other experiments, the pipette solution contained no ADPR and 4.8 mM instead of 8.3 mM $CaCl_2$, giving a free [Ca^{2+}] of ~100 nM. The standard bath solution contained 140 mM NaCl, 2 mM $CaCl_2$, 1 mM $MgCl_2$, and 10 mM HEPES (pH 7.4 with NaOH). For Na^+- and Ca^{2+}-free conditions, the bath solution contained 140 mM *N*-methyl-D-glucamine-Cl (NMDG-Cl), 1 mM $MgCl_2$ and 10 mM HEPES (pH 7.4 with HCl). Single-channel amplitudes were calculated from current traces of 2–10 s duration using amplitude histograms fitted to Gaussian functions. All pooled data from patch-clamp experiments are expressed as means ± s.e.m. from *n* cells. Significant difference was tested by one-way ANOVA.

Calcium measurements

Measurements of the intracellular Ca^{2+} concentration ($[Ca^{2+}]_i$) in single TRPM2-transfected cells were carried out using the fluorescent indicator fura-2 in combination with a monochromator-based imaging system (T.I.L.L. Photonics, Gräfelfing, Germany) attached to an inverted microscope (Axiovert 100, Zeiss, Jena, Germany). HEK293 cells were loaded with 4 μM fura-2-AM (Molecular Probes, Leiden, The Netherlands) supplemented with 0.01% Pluronic F127 for 60 min at 37°C in a standard solution containing 138 mM NaCl, 6 mM KCl, 1 mM $MgCl_2$, 2 mM $CaCl_2$, 5.5 mM glucose and 10 mM HEPES (adjusted to pH 7.4 with NaOH). For $[Ca^{2+}]_i$ measurements, fluorescence was excited at 340 and

380 nm. After correction for the individual background fluorescence, the fluorescence ratio F_{340}/F_{380} was calculated.

Measurements of $[Ca^{2+}]_i$ were carried out on TRPM8-transfected HEK293 cells grown in 96-well microplates. Cells were loaded with 1 μM fluo-4 (Molecular Probes, Leiden, The Netherlands) for 30 min at 37°C in a standard solution (see above). Subsequently, the standard solution was exchanged for a solution containing 1 mM EGTA instead of 2 mM $CaCl_2$, and plates were inserted into a fluorometric-imaging plate reader (Mithras LB 940, Berthold Technologies, Bad Wildbach, Germany). The fluorescence was excited at 485 nm, emitted at 535 nm and corrected for the background fluorescence. Fluorescence values (percentage of initial fluorescence) were measured after addition of ACA, menthol and 3 mM $CaCl_2$ to the EGTA-containing solution. ACA, menthol and 3 mM $CaCl_2$ were applied consecutively in the given order with a time delay of 2 min between each application.

Chemicals

ACA and arachidonyl trifluoromethyl ketone ($AACOCF_3$) were obtained from Calbiochem. ADPR, *N*[3-(trifluoromethyl)-phenyl]anthranilic acid (FFA), 2,4′-dibromoacetophenone (*p*-bromophenacyl bromide (BPB)), H_2O_2, menthol and all other chemicals were obtained from Sigma (Steinheim, Germany). ACA, FFA, $AACOCF_3$ and BPB were dissolved in dimethylsulfoxide (DMSO) giving stock solutions of 50 mM. Menthol was dissolved in ethanol giving a stock solution of 1 M. In final solutions, the concentrations of DMSO and ethanol did not exceed 0.2 and 0.1%, respectively. At these concentrations neither DMSO nor ethanol had any effect on whole-cell currents in HEK293 cells. ADPR was dissolved in distilled water giving a stock solution of 100 mM.

Results

Effects of ACA and FFA on TRPM2

ACA (Figure 1e), belonging to the class of *N*-cinnamoyl-anthranilic acids, has been shown to reduce stimulated arachidonic acid accumulation and insulin secretion in pancreatic islets (Konrad *et al*., 1992; Simonsson *et al*., 1998). We studied the effect of ACA on HEK293 cells transiently transfected with hTRPM2. To provide a maximal activation of TRPM2 in whole-cell patch-clamp experiments, the intracellular pipette solution contained 1 mM ADPR and a free $[Ca^{2+}]_i$ of ~600 nM (buffered with 10 mM BAPTA). Figure 1a shows the rapid development of inward and outward currents within 6–10 s after attaining the whole-cell configuration due to infusion of ADPR. The mean ADPR-induced currents were -995 ± 217 and $+1087\pm209$ pA ($n=6$) at -80 and $+80$ mV, respectively. External application of 20 μM ACA induced a suppression of currents to values of $+4\pm2$ and $+58\pm16$ pA ($n=6$) at -80 and $+80$ mV, respectively. The amplitude of currents was restored to 70 ± 3% of its original value after 2–3 min of washing ($n=6$). Current–voltage relationships were linear throughout the exposure to ACA, suggesting that the ACA-induced block was not voltage-dependent under these conditions (Figure 1b). Application of 20 μM ACA to non-transfected, ADPR-infused HEK293 cells (Figure 1c and d) changed current amplitudes from $+7\pm1$ and $+65\pm22$ pA to $+5\pm1$ and $+44\pm14$ pA ($n=5$) at -80 and $+80$ mV, respectively. This indicates, that our HEK293 cells showed nearly no background current and that ACA completely suppressed TRPM2-mediated currents. Previously, another anthranilic acid derivative, *N*-[3-(trifluoromethyl)-phenyl]anthranilic acid (FFA; Figure 1f) has been introduced as an inhibitor of TRPM2 (Hill *et al*., 2004a). In this study, FFA produced a complete block at concentrations from 50 to 1000 μM, whereas lower concentrations have not been tested so far. To compare the blocking efficacy of FFA and ACA, we subsequently applied 20 μM of either substance to TRPM2-expressing cells. Figure 1g shows the time course of currents during consecutive application of FFA and ACA ($n=3$) and vice versa ($n=3$). Whereas ACA completely suppressed ADPR-induced currents, application of FFA for 60 s induced only a partial inhibition. From individual measurements using either FFA or ACA we determined the time to establish a 50% block. The time to half-block was 24 ± 7 s ($n=5$) and 14 ± 2 s ($n=6$) for FFA (20 μM) and ACA (20 μM), respectively.

Effects of other PLA_2 inhibitors on TRPM2

To verify a possible suppression of TRPM2 activity by inhibition of PLA_2, we tested $AACOCF_3$ and BPB, two PLA_2 inhibitors structurally unrelated to ACA (Figure 2a). Application of 20 μM $AACOCF_3$ ($n=6$) or 100 μM BPB ($n=6$) produced only a very slight or no reduction of ADPR-induced current responses (Figure 2b and c). Subsequent application of ACA completely blocked these currents, suggesting that an ACA-induced TRPM2 block is unrelated to PLA_2 inhibition.

ACA inhibits TRPM2 channels concentration dependently

Application of 1 μM ACA for 4–6 min induced a very slow block which could not be restored after 3–5 min of washing (Figure 3a). Treatment with 1 μM ACA for 4 min ($n=6$) changed current amplitudes from -768 ± 201 to -221 ± 35 pA (at -80 mV) and from $+870\pm226$ to $+299\pm52$ pA (at $+80$ mV). At 1 μM ACA, TRPM2-mediated currents were inhibited by 68 ± 3% (-80 mV) and 63 ± 3% ($+80$ mV), whereas 20 μM ACA produced a block by 100% (-80 mV) and 94 ± 1% ($+80$ mV) (Figure 3b). At 1 μM ACA, the time to establish a 50% block was 127 ± 35 s ($n=6$). To determine a concentration–response relationship for ACA-induced block of TRPM2, we performed calcium-imaging experiments in hTRPM2-transfected HEK293 cells using extracellular H_2O_2 as activator. Application of 5 mM H_2O_2 induced an increase in $[Ca^{2+}]_i$ in TRPM2-transfected cells within 60–80 s after start of application, whereas the responses in TRPM2-transfected cells, treated with 20 μM ACA 3 min before stimulation with H_2O_2, were almost completely abolished (Figure 3c). The concentration of ACA for half-maximal inhibition (IC_{50}) of TRPM2 was 1.7 μM (Figure 3d).

Properties of ACA-mediated block of TRPM2

Intracellular application of FFA has been shown to be ineffective in blocking TRPM2 channels (Hill *et al*., 2004a). We therefore tested the effect of intracellular ACA and applied 50 μM of the substance to the internal face of the plasma membrane *via* the patch pipette. Current development was

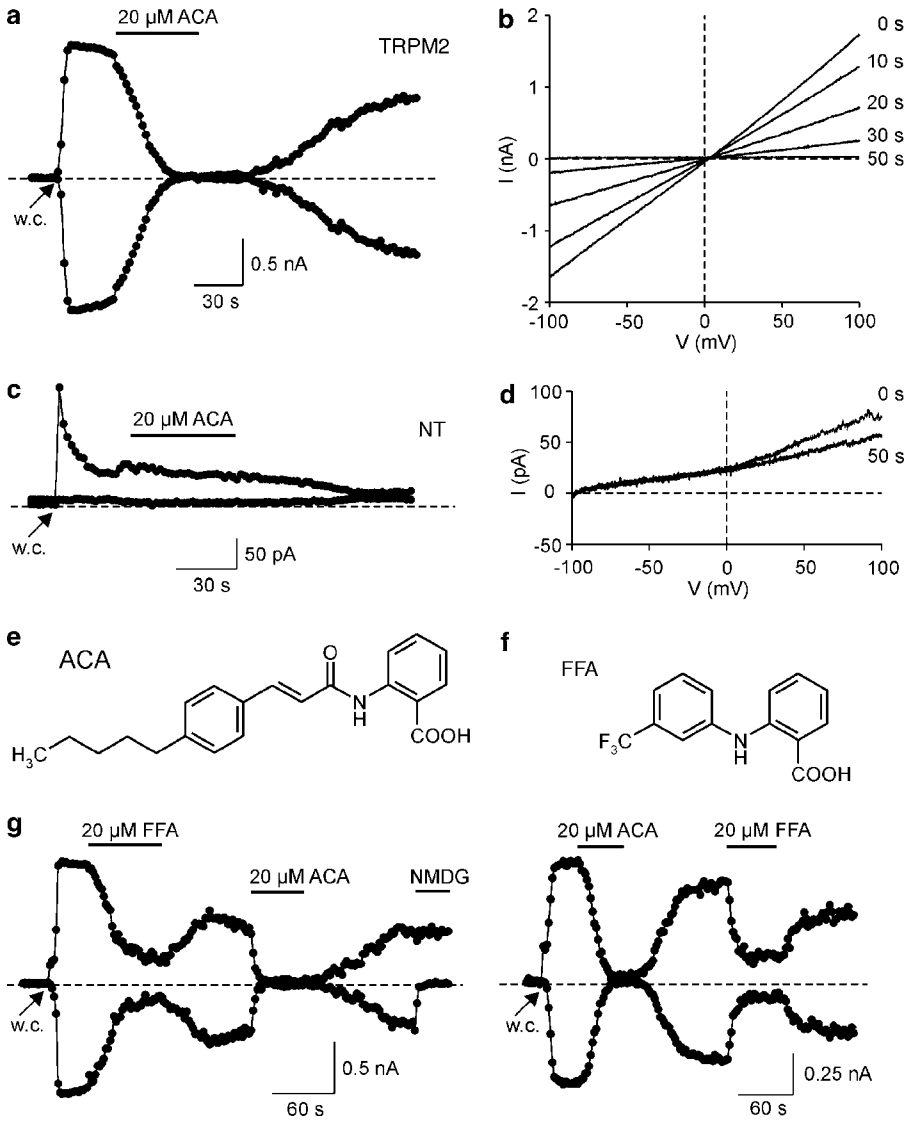

Figure 1 Activation of human TRPM2 currents by ADP-ribose and inhibiton by ACA and FFA. (a) Currents were evoked after obtaining the whole-cell (w.c.) configuration due to infusion of a pipette solution containing 1 mM ADPR. The time course of currents at −80 and +80 mV were obtained from responses during voltage ramps from −100 to +100 mV. (b) Current–voltage relationships from the TRPM2-expressing cell were obtained at different time points following addition of ACA. (c) Nontransfected HEK293 cells showed no development of TRPM2-like, symmetric current pattern upon infusion with ADPR-containing pipette solution. (d) Current–voltage relationships from the nontransfected cell were obtained at different time points following addition of ACA. (e) Chemical structure of ACA. (f) Chemical structure of another TRPM2 antagonist FFA. (g) Extracellular application of 20 μM FFA to a TRPM2-expressing cell partially inhibited inward and outward currents (left trace). After washout of FFA, addition of 20 μM ACA induced a complete block of currents. The cationic nature of inward currents was checked by the exchange of Na^+- and Ca^{2+}-containing bath solution by an $NMDG^+$-containing solution. Application of 20 μM FFA following block by ACA also induced a partial inhibition (right trace).

unchanged in comparison to experiments without intracellular ACA ($n=5$), indicating that ACA is also unable to block TRPM2 from the cytoplasmic side (Figure 4a). Subsequent application of extracellular ACA (20 μM) reversibly blocked the currents, similarly to that seen in cells lacking intracellular ACA.

Furthermore, Hill *et al.* (2004a) showed that the FFA-induced block was much faster at lower extracellular pH, probably due to a reduced fraction of negatively charged FFA. We also tested the effect of pH 6.0 on inhibition of TRPM2 by 1 μM ACA. Under these conditions, the rate of block was speeded and inhibiton was complete (Figure 4b). The time to establish a 50% block was 36 ± 7 s ($n=6$) and thus 3.5-fold faster than at pH 7.4. Interestingly, currents did not recover when ACA was washed out for 1–2 min at pH 6.0, but reappeared immediately after switching to pH 7.4 (Figure 4b). The restored current was again inhibited after application of pH 6.0. This suggests a dependence of both blocking rate and current recovery on pH.

In a next step, effects of ACA were studied on single TRPM2 channels. Single-channel currents were measured in the whole-cell configuration with 1 mM ADPR as intracellular agonist. We used cells with a relatively low TRPM2 expression by selecting those showing a weak fluorescence after transfec-

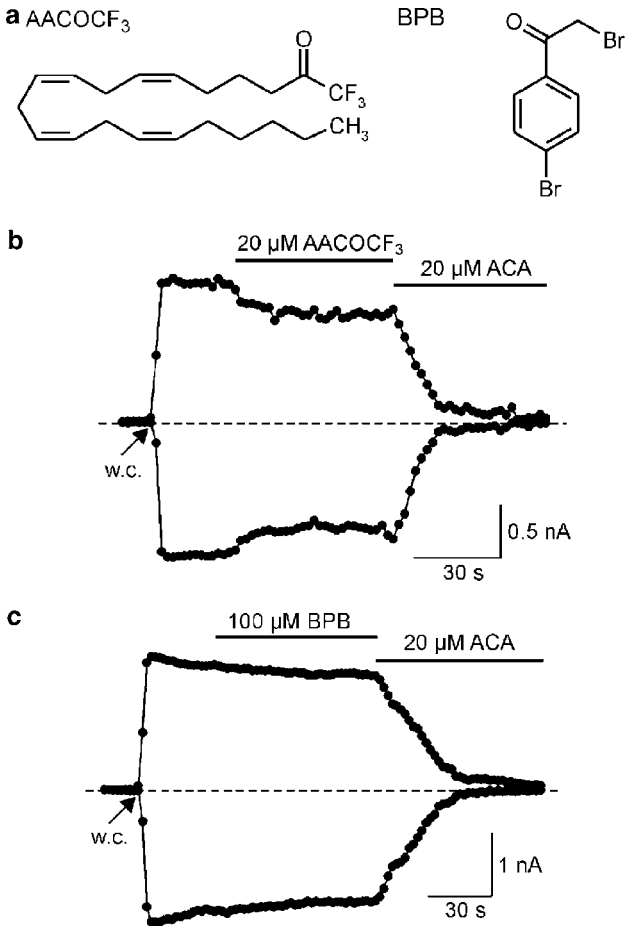

Figure 2 Effects of different phospholipase A_2 inhibitors on TRPM2-mediated currents in HEK293 cells. (a) Chemical structures of the phospholipase A_2 inhibitors $AACOCF_3$ and BPB. (b) Currents were evoked by obtaining the whole-cell (w.c.) configuration and infusion of a pipette solution containing 1 mM ADPR. Currents at −80 and +80 mV were only slightly affected by application of 20 μM $AACOCF_3$ but completely inhibited by subsequent application of 20 μM ACA. (c) ADPR-induced currents were unchanged in the presence of 100 μM BPB but completely inhibited by application of 20 μM ACA.

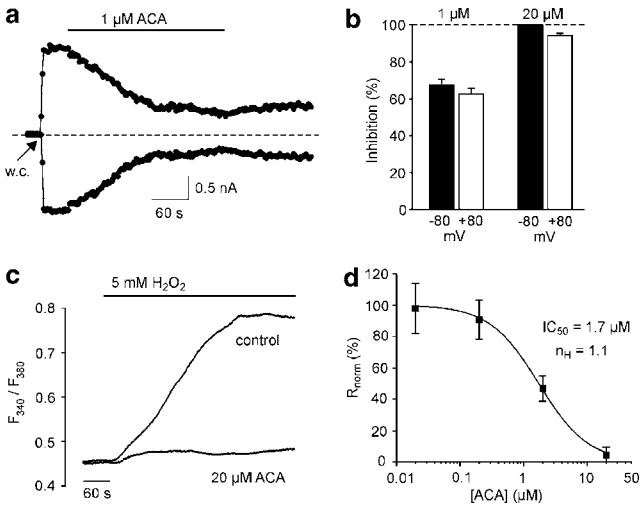

Figure 3 Concentration-dependent inhibition of ADPR-induced currents and H_2O_2-evoked increases in $[Ca^{2+}]_i$ in TRPM2-transfected HEK293 cells by ACA. (a) Currents were evoked after obtaining the whole-cell (w.c.) configuration due to infusion of a pipette solution containing 1 mM ADPR. Currents at −80 and +80 mV were slowly inhibited by application of 1 μM ACA. (b) Concentration dependence of ACA-induced block (means ± s.e.m. from $n = 6$ each) was calculated from current amplitudes at −80 and +80 mV immediately before and 1 min (20 μM) or 4 min (1 μM) after addition of ACA. (c) Effect of 5 mM H_2O_2 on $[Ca^{2+}]_i$ in TRPM2-transfected cells in the absence (control; $n = 8$) and presence of 20 μM ACA ($n = 4$). Shown are mean values from n independent experiments with at least 25 cells each. (d) Concentration-inhibition curve for ACA on H_2O_2-evoked increases in $[Ca^{2+}]_i$ in TRPM2-transfected cells. Data points (mean ± s.e.m. of $n = 3$–4 independent experiments with at least 25 cells each) were calculated from the H_2O_2-induced responses 450 s after application of ACA. The curve was fitted to the logistic function $R_{norm} = 1/\{1 + ([ACA]/IC_{50})^{n}\}$, where R_{norm} is the fluorescence ratio F_{340}/F_{380} in the presence of ACA normalized to that in control conditions, IC_{50} the concentration resulting in half-maximal inhibiton and n_H the Hill coefficient.

tion with the hTRPM2–YFP construct. Under these conditions, channel activity could be resolved even when whole-cell inward current amplitude reached up to −100 pA at −70 mV. Single-channel currents were characterized by an amplitude ranging from −4 to −5.5 pA with a mean value of −4.7 ± 0.5 pA at −70 mV ($n = 12$), corresponding to a chord conductance of 67 pS. Single-channel events with a similar conductance were never observed in nontransfected cells. Extracellular application of 20 μM ACA decreased channel open times without an obvious change of current amplitudes (Figure 5a and b). To characterize the gating behavior of TRPM2 channels in more detail and to quantify a possible rundown of channel activity, we compared mean inward current (I_{mean}) amplitudes during maximal current activation (0 s) and following application of ACA for 50 s ($n = 6$; Figure 5c). Control experiments were performed in the absence of ACA ($n = 6$). I_{mean} was calculated from traces of 10 s duration by averaging the current amplitudes and subtracting the previously determined background current. Background currents at −70 mV were between −4 and −10 pA. The amplitudes of I_{mean} at 0 s for experiments in the presence and absence of ACA were −76 ± 29 and −62 ± 22 pA, respectively. In the absence of ACA, I_{mean} declined over 50 s to 85 ± 12% of its original value. In contrast, application of ACA for 50 s induced a reduction of I_{mean} to 6 ± 2% (Figure 5d). Thus, rundown of TRPM2 activity is significantly slower than block by 20 μM ACA ($P < 0.0001$). To support the observation that a reduction in I_{mean} is due to changes in channel open probability rather than a decrease of single-channel conductance, we calculated the amplitude of single-channel currents from the previous experiments (Figure 5d). Single-channel amplitudes at −70 mV were −4.6 ± 0.8 and −4.8 ± 0.5 pA ($n = 6$) in the absence and presence of ACA, respectively. Thus, a significant change in single-channel conductance could not be observed, which implies that the inhibition of inward currents is rather due to a decrease of TRPM2 open probability.

Effects of ACA on other TRP channels

We tested the ability of ACA for blocking TRP isoforms other than TRPM2, including the closely related channel TRPM8 and the more distantly related channel TRPC6. We first tested the cold- and menthol-sensitive channel TRPM8, which shows the highest sequence identity to TRPM2. External application of 1 mM menthol on hTRPM8-transfected HEK293 cells

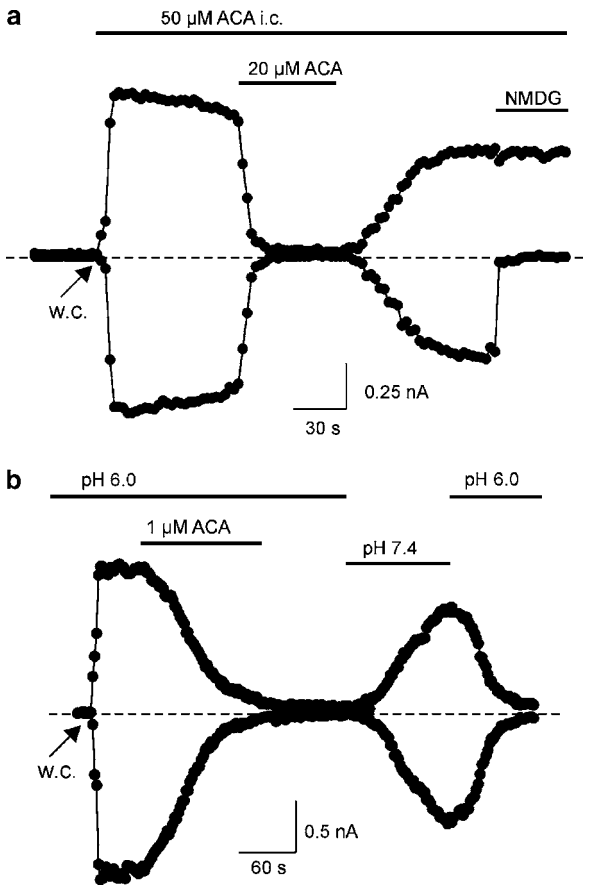

Figure 4 Block of TRPM2 by ACA occurs *via* an extracellular site and is pH dependent. (a) Currents at −80 and +80 mV were evoked by obtaining the whole-cell (w.c.) configuration and infusion of a pipette solution containing 1 mM ADPR. Extracellular application of 20 μM ACA completely inhibited ADPR-induced inward and outward currents, whereas intracellular (i.c.) application of 50 μM ACA had no effect. (b) ADPR-induced currents were completely blocked by 1 μM ACA at pH 6.0. During washout, ADPR-induced currents reappeared immediately after switching to pH 7.4. The restored current was again inhibited after application of pH 6.0.

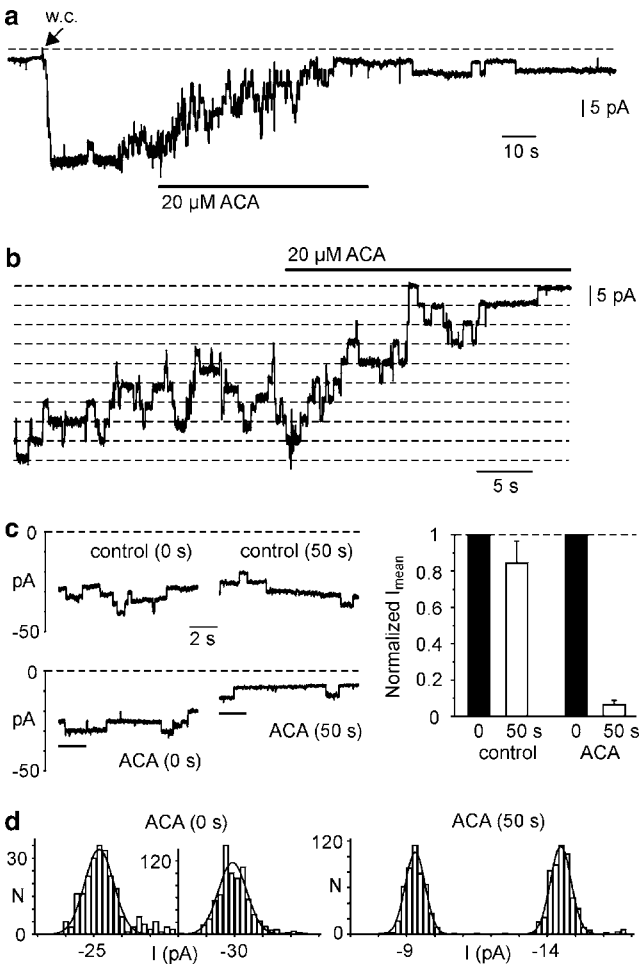

Figure 5 Effect of ACA on TRPM2-mediated single-channel currents in whole-cell (w.c.) recordings. (a) Currents at −70 mV were evoked by obtaining the w.c. configuration and infusion of a pipette solution containing 1 mM ADPR. Extracellular application of 20 μM ACA decreased inward currents. (b) Currents at −70 mV recorded from another cell showed a reduction of channel open states (downward deflections) but no obvious reduction of single-channel amplitude. (c) Current traces of 10 s duration were recorded at −70 mV during maximal current activation (0 s) and following application of ACA for 50 s or in the absence of ACA (control, 50 s). Mean inward current amplitudes (I_{mean}) were calculated from 10 s traces as shown on the left side. I_{mean} at 50 s was normalized to the values at 0 s and is shown as mean ± s.e.m. of $n=6$ cells, each. (d) Amplitude histograms were calculated from 2 s intervals shown in (c) (lower panel, marked by bars). The resulting single-channel currents for this recording were −4.7 pA (ACA, 0 s) and −5.2 pA (ACA, 50 s).

resulted in a rapid activation of inward and outward currents, reaching a plateau phase within 30 s of treatment (Figure 6a). Addition of 20 μM ACA led to a suppression of inward currents from −395±96 to +2±1 pA and of outward currents from +2004±288 to +88±11 pA ($n=5$). Inward currents were restored to 29±1% of its original value after 2–3 min of washing. The time to establish a 50% block of outward currents was 10±2 s ($n=5$). As shown for TRPM2, we tested the ability of the PLA_2 inhibitor BPB to suppress TRPM8 activity. Extracellular application of 100 μM BPB ($n=5$) did not significantly reduce menthol-induced currents (Figure 6b), suggesting a PLA_2-independent effect of ACA on TRPM8. Measurements of $[Ca^{2+}]_i$ using a fluorometric imaging plate reader showed a concentration-dependent inhibiton of menthol-induced fluorescence signals by ACA (Figure 6c). The IC_{50} values for the inhibition of TRPM8 activity yielded from ACA/menthol-induced responses and menthol-induced responses corrected for ACA-dependent signals were 5.4 and 3.9 μM, respectively.

Whole-cell currents through hTRPC6 were evoked after attaining the whole-cell configuration due to infusion of 30 μM AlF_4^- added to the pipette solution (Figure 7a). Extracellular application of 20 μM ACA induced an inhibition of inward and outward current amplitudes from −449±145 to −31±14 pA and +551±98 to +117±31 pA ($n=7$), respectively. The time to establish a 50% block of outward currents was 12±3 s ($n=7$). Application of 100 μM BPB ($n=5$) was not sufficient to reduce TRPC6-mediated currents (Figure 7b). Subsequently applied ACA inhibited these currents, suggesting that ACA blocks TRPC6 not *via* PLA_2 modulation. Endogenous currents in nontransfected, AlF_4^--infused HEK293 cells ($n=6$) were sensitive to NMDG, but were largely insensitive to ACA and showed only very small amplitudes (Figure 7c). Therefore, a considerable contribution of endogenous currents to the

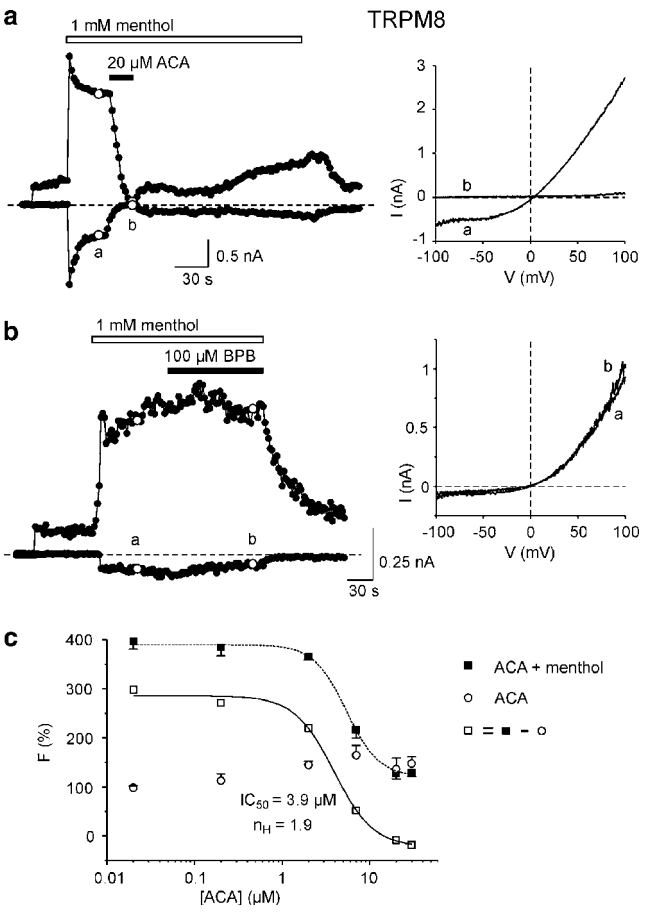

Figure 6 Inhibition of human TRPM8 channels by ACA. (a) Currents through TRPM8 were activated by 1 mM menthol. The time course of currents at −80 and +80 mV yielded from responses during voltage ramps from −100 to +100 mV. Extracellular application of 20 μM ACA inhibited both inward and outward currents. Current–voltage relationships were recorded at the time points *a* and *b*. (b) Application of the PLA_2-inhibitor BPB did not inhibit menthol-induced currents. Current–voltage relationships were recorded at the time points *a* and *b*. (c) Concentration-inhibition curve for ACA on menthol-evoked increases in $[Ca^{2+}]_i$ in TRPM8-transfected cells. $[Ca^{2+}]_i$ responses were either measured as changes in fluorescence intensity (*F*) before and 30 min after the addition of ACA, 1 mM menthol and Ca^{2+} (mean±s.e.m. of $n=6$–8 independent experiments for each concentration) or as changes in *F* before and 30 min after addition of ACA and Ca^{2+} to a Ca^{2+}-free solution (mean±s.e.m. of $n=4$ independent experiments for each concentration). Data points for menthol-induced responses were calculated by subtracting mean *F* values in the presence of ACA and the absence of menthol from the respective values in the presence of both ACA and 1 mM menthol. The curves were fitted to the logistic function $F=F_{min}+(F_{max}-F_{min})/\{1+([ACA]/IC_{50})^n\}$. The concentrations of ACA giving a half-maximal inhibitory effect (IC_{50}) were 5.4 and 3.9 μM for menthol/ACA-induced and menthol-induced responses, respectively. The respective Hill coefficients n_H were 2.3 and 1.9.

activity of TRPC6-transfected cells can be excluded. The IC_{50} value for the inhibition of AlF_4^--induced TRPC6 currents was 2.3 μM (Figure 7d), quite similar to the potencies of ACA in inhibiting TRPM2 and TRPM8 activity.

ACA inhibits native TRPM2 channels in U937 cells

To compare main properties of ACA-induced channel inhibition in heterologous and native expression systems, we chose the human histiocytic lymphoma cell line U937, which has been reported to express ADPR-gated cation channels and TRPM2 mRNA (Perraud *et al*., 2001; Sano *et al*., 2001). We verified the expression of the TRPM2 protein in this cell line by generating a specific antibody. Polyclonal antisera were tested using membrane fractions of HEK293 cells transiently transfected with hTRPM3 (Grimm *et al*., 2003) or hTRPM2 (Figure 8a). The expressed protein detected by the antibody showed a molecular weight approximating the calculated value for TRPM2 of 170 kDA. The antiserum tested was subsequently used to detect TRPM2 expression in U937 cells and in the human myelocytic cell line HL-60 (Figure 8b). In membranes of the human megakaryoblastic cell line MEG-01, TRPM2 could not be detected (Figure 8b). Whole-cell recordings in U937 cells were performed in analogy to measurements in TRPM2-transfected HEK293 cells. Figure 8c shows the rapid development of inward and outward currents within 6–10 s after attaining the whole-cell configuration due to infusion of ADPR. The mean amplitudes of these currents were −1419±42 and +1403±41 pA ($n=4$) at −80 and +80 mV, respectively. The ACA-induced block showed no voltage dependence (Figure 8c) and was 100% and 97±1% for inward and outward currents, respectively. Currents were completely restored to their original values after 1 min of washing ($n=4$). The time to establish a 50% block was 10±1 s ($n=4$) and not statistically different from the value for recombinant TRPM2 channels (Figure 8d). In summary, ACA is an effective inhibitor of TRPM2 in heterologously and natively expressing cells.

Discussion

Our results suggest that ACA blocks TRPM2, but that this effect is mainly independent of inhibition of PLA_2. First, two other PLA_2 inhibitors had almost no effect on TRPM2-mediated currents. Second, intracellularly applied ACA was ineffective in modulating TRPM2 activity. Third, the IC_{50} value of 1.7 μM and the full block at 20 μM are below those ACA concentrations ($\geqslant 50\,\mu$M) required for a significant inhibition of PLA_2 activity in pancreatic islets (Konrad *et al*., 1992; Simonsson *et al*., 1998). Fourth, the comparable block of ACA (10 μM) and antisense nucleotide treatment against cytoplasmic PLA_2 on Ca^{2+}-evoked exocytosis in insulinoma cells (Olsen *et al*., 2003) could also be explained by an ACA-induced inhibition of Ca^{2+} entry, which in turn stimulates cytoplasmic PLA_2. Interestingly, many studies that use ACA to ascertain PLA_2 involvement are conducted in pancreatic islet and insulinoma cells, which both express TRPM2 (Hara *et al*., 2002; Qian *et al*., 2002) and possibly other ACA-sensitive channels. It can therefore not be excluded, that ACA inhibits Ca^{2+}-dependent PLA_2 activity by blocking TRP or other Ca^{2+}-permeable channels.

Recently, it has been shown that another anthranilic acid derivative, FFA, completely inhibits recombinant hTRPM2 channels at concentrations $\geqslant 50\,\mu$M (Hill *et al*., 2004a). It should be noted that anthranilic acid alone had no effect on TRPM2 activity (R. Kraft, unpublished observations). Two further substances, clotrimazole and econazole, have been described to inhibit TRPM2 currents at 3–30 μM (Hill *et al*., 2004b), suggesting an IC_{50} value close to that for TRPM2 inhibition by ACA. Some properties of block induced by FFA,

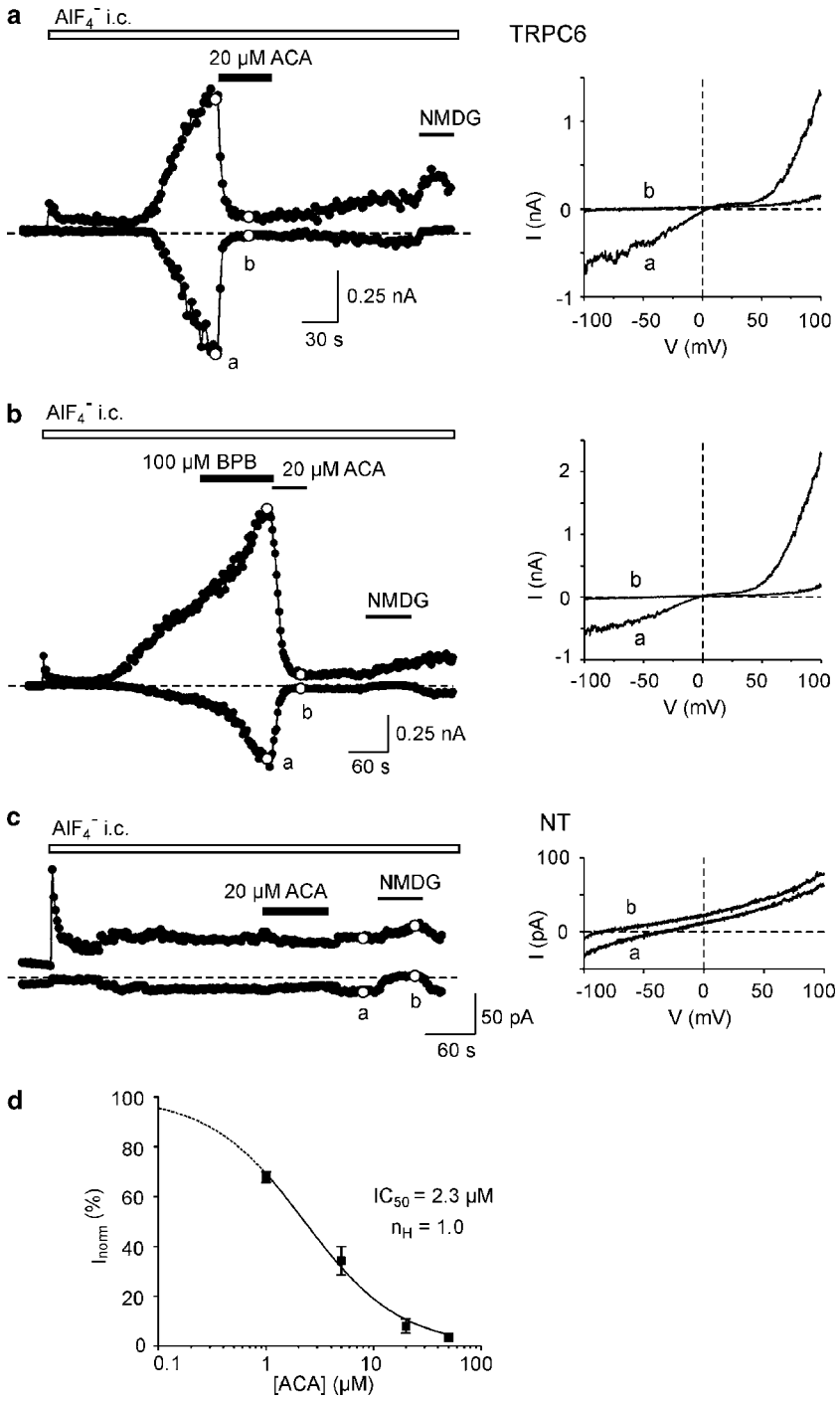

Figure 7 Inhibition of human TRPC6 channels by ACA. (a) Currents through TRPC6 were evoked by obtaining the whole-cell (w.c.) configuration and infusion of a pipette solution containing 30 μM AlF_4^-. The time course of currents at -80 and $+80$ mV yielded from responses during voltage ramps from -100 to $+100$ mV. Extracellular application of 20 μM ACA led to a reduction of both inward and outward currents. Exchange of the Na^+- and Ca^{2+}-containing bath solution by an $NMDG^+$-containing solution abolished inward currents. Current–voltage relationships were recorded at the time points *a* and *b*. (b) Application of the PLA_2-inhibitor BPB did not inhibit w.c. currents, whereas subsequent application of ACA blocked TRPC6 activity. Current–voltage relationships were recorded at the time points *a* and *b*. (c) Concentration-inhibition curve for ACA on AlF_4^--evoked inward currents in TRPC6-transfected cells. Data points (mean $\pm$ s.e.m. of $n = 5$–7 cells for each concentration) were calculated from current responses before and after application of 1, 5, 20 and 50 μM ACA. The curve was fitted to the logistic function $I_{norm} = 1/\{1 + ([ACA]/IC_{50})^n\}$, where I_{norm} is the current amplitude at -80 mV in the presence of ACA normalized to that in control conditions, IC_{50} the concentration resulting in half-maximal inhibiton and n_H the Hill coefficient.

clotrimazole and econazole were also observed for ACA-mediated inhibition. Most notably, at lower concentrations the rate of inhibition was drastically slowed (Hill *et al*., 2004a, b). At 1 μM, ACA showed a very slow block requiring nearly 130 s for a 50% reduction of current amplitudes. At 20 μM ACA, the corresponding value was about 10-fold smaller. The inhibition

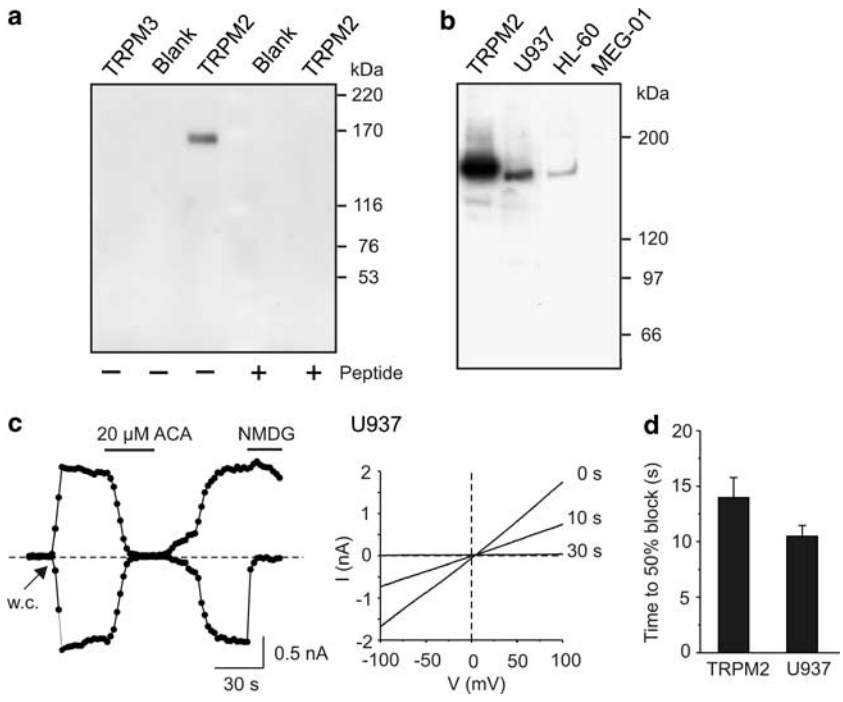

Figure 8 ACA inhibits TRPM2 currents in human U937 cells. (a) Membrane proteins (4 μg) from nontransfected cells (Blank), hTRPM3-transfected and hTRPM2-transfected HEK293 cells were used for characterization of the TRPM2 antibody. The specificity of the antibody reaction was verified by incubating parallel lanes with the antibody in the presence of the peptide used for immunization. (b) Membrane proteins from U937, HL-60, MEG-01 cells (20 μg each) and from hTRPM2-transfected HEK293 cells (4 μg) were used for Western blot analysis. (c) Currents were evoked after obtaining the whole-cell (w.c) configuration due to infusion of a pipette solution containing 1 mM ADPR. Application of 20 μM ACA inhibited both inward and outward currents. Exchange of the Na^+- and Ca^{2+}-containing bath solution by an $NMDG^+$-containing solution suppressed inward currents. Current–voltage relationships were obtained at different time points following addition of ACA. (d) The graph shows the mean times $\pm$ s.e.m. required to produce a 50% reduction of ADPR-induced currents by 20 μM ACA in hTRPM2-transfected HEK293 cells ($n=6$) and U937 cells ($n=4$).

by 1 μM ACA was accelerated by decreasing pH from 7.4 to 6.0. We assume that ACA (as well as FFA) is a weak acid, which is mainly present in the negatively charged form at pH 7.4. At pH 6.0, we therefore expect a higher level of the uncharged molecule, which may be responsible for the fast block of TRPM2. The reduction of channel open probability and the lack of voltage dependency of the block furthermore suggest an inhibition of TRPM2 activity by modulating channel gating.

Two other human members of the TRP superfamily, that is the closely related channel TRPM8 and the more distantly related channel TRPC6, were also tested on ACA sensitivity. ACA (20 μM) led to a nearly complete inhibition of TRPC6-mediated currents and a full suppression of TRPM8 activity, suggesting that effects of ACA are not unique to TRPM2 or the TRPM subfamily. A modulation of TRP channel currents by ACA in general was supported by inhibitory as well as stimulatory effects on TRPC3, TRPC5, TRPV1 and TRPV4 (R. Kraft, unpublished observations). Thus, ACA also represents a TRPM8 blocker with a IC_{50} value of 3.9 μM, which is comparable to potencies of the recently described TRPM8 (and TRPV1) antagonists BCTC, thio-BCTC and capsazepine (Behrendt *et al*., 2004). The interaction of ACA with the more distantly related channel TRPC6 adds this substance to a group of other 'unspecific' TRP channel modulators, including lanthanides (La^{3+} and Gd^{3+}), 2-aminoethoxydiphenyl borate (2-APB) and FFA. One important feature of these substances is their differential modulation of single TRP members or TRP subgroups: TRPM2, for instance, is blocked by FFA (Hill *et al*., 2004a) and ACA (this study), but is resistant to lanthanides (Kraft *et al*., 2004; Xu *et al*., 2005) and 2-APB (Xu *et al*., 2005). TRPC6 has been shown to be blocked by 2-APB (Xu *et al*., 2005), ACA (this study) and lanthanides (Inoue *et al*., 2001; Jung *et al*., 2002), but to be potentiated by FFA (Inoue *et al*., 2001; Jung *et al*., 2002). The resultant pattern of TRPM2 and TRPC6 modulation by the 'unspecific' compounds La^{3+} (or Gd^{3+}), 2-APB, FFA and ACA is specific, when comparing both channels. Therefore, the combined use of different 'unspecific' TRP channel blockers or modulators can be helpful for identifying TRP channels in native cells. Indeed, one aim of our further studies is the characterization of TRPM2 function in microglia by using the known blockers FFA, clotrimazole and ACA.

In conclusion, we show that ACA modulates different TRP channels most probably by a direct interaction. Owing to its high potency and efficacy on TRPM2, ACA can serve, in combination with other blockers, as a pharmacological tool for studying H_2O_2-induced Ca^{2+} signalling and biological functions of TRPM2 channels in native cells.

We thank Inge Reinsch for technical assistance and Michael Schaefer for providing hTRPM8 cDNA. We are supported by the Deutsche Forschungsgemeinschaft, Fonds der Chemischen Industrie and Sonnenfeld-Stiftung.

References

BEHRENDT, H.J., GERMANN, T., GILLEN, C., HATT, H. & JOSTOCK, R. (2004). Characterization of the mouse cold-menthol receptor TRPM8 and vanilloid receptor type-1 VR1 using a fluorometric imaging plate reader (FLIPR) assay. *Br. J. Pharmacol.,* **141,** 737–745.

FLEIG, A. & PENNER, R. (2004). The TRPM ion channel subfamily: molecular, biophysical and functional features. *Trends Pharmacol. Sci.,* **25,** 633–639.

FONFRIA, E., MARSHALL, I.C., BENHAM, C.D., BOYFIELD, I., BROWN, J.D., HILL, K., HUGHES, J.P., SKAPER, S.D. & MCNULTY, S. (2004). TRPM2 channel opening in response to oxidative stress is dependent on activation of poly(ADP-ribose) polymerase. *Br. J. Pharmacol.,* **143,** 186–192.

FONFRIA, E., MARSHALL, I.C., BOYFIELD, I., SKAPER, S.D., HUGHES, J.P., OWEN, D.E., ZHANG, W., MILLER, B.A., BENHAM, C.D. & MCNULTY, S. (2005). Amyloid beta-peptide(1-42) and hydrogen peroxide-induced toxicity are mediated by TRPM2 in rat primary striatal cultures. *J. Neurochem.,* **95,** 715–723.

GRIMM, C., KRAFT, R., SAUERBRUCH, S., SCHULTZ, G. & HARTENECK, C. (2003). Molecular and functional characterization of the melastatin-related cation channel TRPM3. *J. Biol. Chem.,* **278,** 21493–21501.

HARA, Y., WAKAMORI, M., ISHII, M., MAENO, E., NISHIDA, M., YOSHIDA, T., YAMADA, H., SHIMIZU, S., MORI, E., KUDOH, J., SHIMIZU, N., KUROSE, H., OKADA, Y., IMOTO, K. & MORI, Y. (2002). LTRPC2 Ca^{2+}-permeable channel activated by changes in redox status confers susceptibility to cell death. *Mol. Cell,* **9,** 163–173.

HEINER, I., EISFELD, J., HALASZOVICH, C.R., WEHAGE, E., JÜNGLING, E., ZITT, C. & LÜCKHOFF, A. (2003a). Expression profile of the transient receptor potential (TRP) family in neutrophil granulocytes: evidence for currents through long TRP channel 2 induced by ADP-ribose and NAD. *Biochem. J.,* **371,** 1045–1053.

HEINER, I., EISFELD, J. & LÜCKHOFF, A. (2003b). Role and regulation of TRP channels in neutrophil granulocytes. *Cell Calcium,* **33,** 533–540.

HILL, K., BENHAM, C.D., MCNULTY, S. & RANDALL, A.D. (2004a). Flufenamic acid is a pH-dependent antagonist of TRPM2 channels. *Neuropharmacology,* **47,** 450–460.

HILL, K., MCNULTY, S. & RANDALL, A.D. (2004b). Inhibition of TRPM2 channels by the antifungal agents clotrimazole and econazole. *Naunyn Schmiedeberg's Arch. Pharmacol.,* **370,** 227–237.

HILL, K., TIGUE, N.J., KELSELL, R.E., BENHAM, C.D., MCNULTY, S., SCHAEFER, M. & RANDALL, A.D. (2006). Characterisation of recombinant rat TRPM2 and a TRPM2-like conductance in cultured rat striatal neurones. *Neuropharmacology,* **50,** 89–97.

INAMURA, K., SANO, Y., MOCHIZUKI, S., YOKOI, H., MIYAKE, A., NOZAWA, K., KITADA, C., MATSUSHIME, H. & FURUICHI, K. (2003). Response to ADP-ribose by activation of TRPM2 in the CRI-G1 insulinoma cell line. *J. Membr. Biol.,* **191,** 201–207.

INOUE, R., OKADA, T., ONOUE, H., HARA, Y., SHIMIZU, S., NAITOH, S., ITO, Y. & MORI, Y. (2001). The transient receptor potential protein homologue TRP6 is the essential component of vascular α_1-adrenoceptor-activated Ca^{2+}-permeable cation channel. *Circ. Res.,* **88,** 325–332.

JUNG, S., STROTMANN, R., SCHULTZ, G. & PLANT, T.D. (2002). TRPC6 is a candidate channel involved in receptor-stimulated cation currents in A7r5 smooth muscle cells. *Am. J. Physiol. Cell. Physiol.,* **282,** C347–C359.

KONRAD, R.J., JOLLY, Y.C., MAJOR, C. & WOLF, B.A. (1992). Inhibition of phospholipase A_2 and insulin secretion in pancreatic islets. *Biochim. Biophys. Acta,* **1135,** 215–220.

KRAFT, R., GRIMM, C., GROSSE, K., HOFFMANN, A., SAUERBRUCH, S., KETTENMANN, H., SCHULTZ, G. & HARTENECK, C. (2004). Hydrogen peroxide and ADP-ribose induce TRPM2-mediated calcium influx and cation currents in microglia. *Am. J. Physiol. Cell. Physiol.,* **286,** C129–C137.

KRAFT, R. & HARTENECK, C. (2005). The mammalian melastatin-related transient receptor potential cation channels: an overview. *Pflügers Arch.,* **451,** 204–211.

MCHUGH, D., FLEMMING, R., XU, S.Z., PERRAUD, A.L. & BEECH, D.J. (2003). Critical intracellular Ca^{2+} dependence of transient receptor potential melastatin 2 (TRPM2) cation channel activation. *J. Biol. Chem.,* **278,** 11002–11006.

NAGAMINE, K., KUDOH, J., MINOSHIMA, S., KAWASAKI, K., ASAKAWA, S., ITO, F. & SHIMIZU, N. (1998). Molecular cloning of a novel putative Ca^{2+} channel protein (TRPC7) highly expressed in brain. *Genomics,* **54,** 124–131.

OLSEN, H.L., NORBY, P.L., HOY, M., SPEE, P., THAMS, P., CAPITO, K., PETERSEN, J.S. & GROMADA, J. (2003). Imidazoline NNC77-0074 stimulates Ca^{2+}-evoked exocytosis in INS-1E cells by a phospholipase A_2-dependent mechanism. *Biochem. Biophys. Res. Commun.,* **303,** 1148–1151.

PERRAUD, A.L., FLEIG, A., DUNN, C.A., BAGLEY, L.A., LAUNAY, P., SCHMITZ, C., STOKES, A.J., ZHU, Q., BESSMAN, M.J., PENNER, R., KINET, J.P. & SCHARENBERG, A.M. (2001). ADP-ribose gating of the calcium-permeable LTRPC2 channel revealed by Nudix motif homology. *Nature,* **411,** 595–599.

PERRAUD, A.L., KNOWLES, H.M. & SCHMITZ, C. (2004). Novel aspects of signaling and ion-homeostasis regulation in immunocytes. The TRPM ion channels and their potential role in modulating the immune response. *Mol. Immunol.,* **41,** 657–673.

QIAN, F., HUANG, P., MA, L., KUZNETSOV, A., TAMARINA, N. & PHILIPSON, L.H (2002). TRP genes: candidates for nonselective cation channels and store-operated channels in insulin-secreting cells. *Diabetes,* **51** (Suppl 1), S183–S189.

SANO, Y., INAMURA, K., MIYAKE, A., MOCHIZUKI, S., YOKOI, H., MATSUSHIME, H. & FURUICHI, K. (2001). Immunocyte Ca^{2+} influx system mediated by LTRPC2. *Science,* **293,** 1327–1330.

SIMONSSON, E., KARLSSON, S. & AHREN, B. (1998). Ca^{2+}-independent phospholipase A_2 contributes to the insulinotropic action of cholecystokinin-8 in rat islets: dissociation from the mechanism of carbachol. *Diabetes,* **47,** 1436–1443.

SMITH, M.A., HERSON, P.S., LEE, K., PINNOCK, R.D. & ASHFORD, M.L. (2003). Hydrogen-peroxide-induced toxicity of rat striatal neurones involves activation of a non-selective cation channel. *J. Physiol.,* **547,** 417–425.

UEMURA, T., KUDOH, J., NODA, S., KANBA, S. & SHIMIZU, N. (2005). Characterization of human and mouse TRPM2 genes: Identification of a novel N-terminal truncated protein specifically expressed in human striatum. *Biochem. Biophys. Res. Commun.,* **328,** 1232–1243.

WEHAGE, E., EISFELD, J., HEINER, I., JÜNGLING, E., ZITT, C. & LÜCKHOFF, A. (2002). Activation of the cation channel long transient receptor potential channel 2 (LTRPC2) by hydrogen peroxide. A splice variant reveals a mode of activation independent of ADP-ribose. *J. Biol. Chem.,* **277,** 23150–23156.

XU, S.Z., ZENG, F., BOULAY, G., GRIMM, C., HARTENECK, C. & BEECH, D.J. (2005). Block of TRPC5 channels by 2-aminoethoxydiphenyl borate: a differential, extracellular and voltage-dependent effect. *Br. J. Pharmacol.,* **145,** 405–414.

ZHANG, W., CHU, X., TONG, Q., CHEUNG, J.Y., CONRAD, K., MASKER, K. & MILLER, B.A. (2003). A novel TRPM2 isoform inhibits calcium influx and susceptibility to cell death. *J. Biol. Chem.,* **278,** 16222–16229.

(Received December 22, 2005
Revised February 16, 2006
Accepted March 3, 2006
Published online 10 April 2006)